J. Am. Chem. Soc. (accepted manuscript)

Reversible Solid-State Isomerism of Azobenzene-Loaded Large-Pore Isoreticular Mg-CUK-1

Junpeng He,† Kanchan Aggarwal,† Naman Katyal,† Shichao He,† Edward Chiang,† Samuel G. Dunning,† Joseph E. Reynolds III,† Alexander Steiner,‡ Graeme Henkelman,*† Emily L. Que*† and Simon M. Humphrey*†

†University of Texas at Austin, Department of Chemistry, Austin, Texas 78712, U.S.A.

‡University of Liverpool, Department of Chemistry, Crown St., Liverpool L69 7ZD, U.K.

ABSTRACT: A large-pore version of Mg-CUK-1, a water-stable MOF with 1-D channels, was synthesized in basic water. MgCUK-1L has a BET surface area of 2,896 m^2 g^{-1} and shows stark selectivity for CO_2 sorption over N_2, O_2, H_2, and CH_4. It displays reversible, multi-step gated sorption of CO_2 below 0.33 atm. The dehydrated single crystal structure of Mg-CUK-1L confirms retention of the open channel structure. The MOF can be loaded with organic molecules by immersion in hot melts, providing single crystals suitable for X-ray diffraction. Trans-azobenzene fills the channels in a 2×2 arrangement. Solid-state UV-Vis spectroscopy reveals that azobenzene molecules undergo reversible trans-cis isomerization, despite being close-packed; this surprising result is confirmed by DFT-simulated UV-vis spectra.

Hydrothermal synthesis of functional metal-organic frameworks (MOFs) using water as the only reaction medium is beneficial from an environmental perspective, and provides MOFs that are inherently moisture-stable.[1] Their application as adsorbents for the capture of potable water in arid regions has been demonstrated by Yaghi and co-workers.[2] MOFs that resist hydrolytic decomposition also hold potential for applications in molecular separation/sequestration of wet feed-gas mixtures.[3]

The M-CUK-1 series of MOFs (M = Mg, Mn, Co, Ni) are prepared under sub-hydrothermal conditions (200–250 °C).[4] They are based on 2,4-pyridine dicarboxylic acid (2,4-pdc; NC_5H_3-2,4-CO_2H) and have a 1-D channel micropore structure. Since their discovery in 2007,[4b] our group and others have shown that M-CUK-1 materials act as high-capacity and highly cyclable water adsorbents for adsorption-driven chiller applications,[4d] and for H_2S capture.[4e] Compared to the d-metal analogues, Mg-CUK1 utilizes a non-toxic metal, can be prepared rapidly at scale (30 min) using microwave-assisted heating, has a lower gravimetric density, and a higher thermal stability (up to 450 °C).[4a] MgCUK-1 selectively adsorbs p-isomers from crude xylenes and divinylbenzenes; single crystal X-ray diffraction (SCXRD) also permitted valuable structural resolution of p-isomer-loaded materials.[4a]

Given the versatility of Mg-CUK-1, we have applied an isoreticular approach[5] to obtain a large-channel ('L') version of Mg-CUK-1, which has a greatly increased surface area and is able to adsorb

azobenzene (AzB) directly from a hot melt, resulting in X-ray quality crystals. Close-packed AzB in Mg-CUK-1L surprisingly undergo reversible cis-trans isomerism.

The ligand 4-(4-carboxyphenyl) picolinic acid (cppH$_2$; $C_5H_3N_2$-CO_2H-4-(C_6H_4-4-CO_2H)) has the same coordinating moieties as 2,4-pdc but is extended by an extra phenyl ring at the 4-position. CppH$_2$ was obtained in gram quantities via Suzuki coupling followed by saponification of the dimethyl ester (Supporting Information). Precipitation with excess HCl yielded cppH$_2$ as the pyridinium hydrochloride salt. Co-dissolution of cppH$_2$·HCl with 1.5 eq. of $Mg(NO_3)_2$ in water containing 3 eq. of KOH resulted in an opaque white slurry, which was heated at 240 °C, yielding colorless crystalline rods of the target MOF.

Mg-CUK-1L, ($[Mg_3(\mu^3\text{-}OH)_2(cpp)_2]\cdot nH_2O$), is isoreticular with the M-CUK-1 materials and crystallizes in the same monoclinic space group (C2/c; Z = 4). The asymmetric unit contains one complete cpp^{2-} ligand bound to two crystallographically-unique Mg(II) centers (Figure 1A). The Mg(II) coordination modes include a five-membered N,C-chelate (N1−Mg1−O1; Figure 1A) that allows cpp^{2-} to act as a linear linker akin to 4,4'-biphenyl, which yielded isoreticular versions of MOF-5.[6] However, unlike the IRMOFs, the asymmetry of cpp^{2-} results in the channel walls of Mg-CUK-1L having a double-walled structure (Figure 1B). In the original M-CUK-1 series, these structural aspects were shown to impart enhanced mechanical and chemical stability.[4]

Mg-CUK-1L has accessible channel openings of 17.3×13.7 Å. Compared to Mg-CUK-1 (10.0×9.5 Å), the channels have a 2.5x greater cross-sectional area (237 vs. 95 Å^2; Figure 1C). The VOID utility in Platon[7] predicts an accessible volume of 2,708 Å^3 cell^{-1}, representing 56% of the cell volume. Thermogravimetric analysis (TGA) of as-synthesized Mg-CUK-1L revealed a mass loss of 18 wt% below 60 °C (Figure S1). Comparison to a predehydrated sample indicates that H_2O undergoes dynamic exchange with ambient moisture (Figure S1, inset). The unusually low dehydration temperature is indicative of hydrophobic microchannels. cpp^{2-} is more hydrophobic than pdc^{2-} and the total amount of H_2O removed from Mg-CUK-1L was slightly less than for Mg-CUK-1. Between 65−480 °C MgCUK-1L lost no further mass (Figure S1); the large window of thermal stability is due to the highly electrostatic nature of Mg^{2+}–O bonds. The TGA-derived mass loss corresponds to n = 7.3 H_2O. Combustion microanalysis was in close agreement, yielding n = 7.1. Solvent O-atoms (Figure 1B) were also directly located in the electron difference map, yielding n = 9.5.

Attempts were made to dehydrate a single crystal of Mg-CUK1L in situ on the diffractometer by increasing the temperature of the N_2 cryostream. This method provided the dehydrated structures of the original M-CUK-1 materials, but single crystals of Mg-CUK-1L fractured upon cooling. Instead, Mg-CUK-1L crystals were pre-dehydrated at 80 °C under vacuum and subsequently used to collect SCXRD data for the dehydrated phase (Figure 2A & Supporting Information). This confirmed that Mg-CUK-1L resisted pore collapse upon dehydration; the material shows a concertina distortion in the crystallographic ab-plane compared to the fully hydrated structure (dimensions = 18.1×12.8 Å; Figures 2, S4 & Table S1), facilitated by changes in the Mg−O bond angles. The cpp^{2-} ligand also offers greater solidstate flexibility compared with the parent CUK-1 series, based on rotation between the pyridyl and phenyl rings within the channel walls (dihedral angle change = +3.1°; from 28.5 to 31.6°). In-line with the hygroscopic nature of Mg-CUK-1L, trace H_2O was always found in the channels upon crystal transfer to the diffractometer, corresponding to n = 1.25; ¼-occupancy O-atoms were only located near the channel walls.

The porosity of Mg-CUK-1L was assessed by collection of adsorption-desorption isotherms between 0.02−0.95 atm. Crystalline samples were activated at 100 °C under vacuum overnight and powder X-ray diffraction analysis (PXRD) confirmed that the bulk structure was retained upon activation and

re-exposure to water (Figures S2 & S3). Mg-CUK-1L showed a clear sorption selectivity for CO_2 over all other gases studied (Figure 3). The maximum measured adsorption capacity for CO_2 was 17.5 mmol g^{-1} at 196 K, corresponding to 56.6 wt%. The estimated BET surface area of Mg-CUK-1L based on CO_2 adsorption data was 2,896 m^2 g^{-1}. The uptake of other gases was lower: 6.15 (CH_4; 196 K), 4.64 (H_2; 77 K), 4.23 (O_2; 77 K) and 2.37 mmol g^{-1} (N_2; 77 K). At p/p_0 = 0.4, the molar sorption selectivity for CO_2/N_2 = 8.1 and CO_2/O_2 = 4.7. While the latter gases showed normal Type-I sorption behavior, CO_2 displayed a multi-step adsorption-desorption process with a pronounced hysteresis (Figure 3; blue data). Between p/p_0 = 0.02−0.33 the adsorption of CO_2 showed two distinct steps prior to saturation. The desorption hysteresis mirrored the adsorption steps, with a remanence of ca. 0.10.

This type of stepped sorption behavior has been observed in MOFs with larger, meso-sized pores,[8] and is commonly attributed to 'gating effects', whereby a framework undergoes dynamic distortion upon loading and unloading.[9] Long and co-workers recently exploited gated CH_4 sorption in a MOF to counteract the normal thermodynamic processes, thus obtaining a larger working capacity.[10] The SCXRD structure of the dehydrated Mg-CUK-1L phase (Figure 2) indicates that a similar dynamic channel breathing effect is at-play. In situ PXRD studies conducted at 0, 0.18 and 0.45 atm CO_2 loading (corresponding to the fully evacuated structure, before the onset of the first gating step, and at the onset of saturation, respectively) confirmed that the bulk material remained crystalline at each stage with a PXRD pattern corresponding to the fully dehydrated phase. However, upon exposure of the CO_2-loaded material to humid air for 1 h, the PXRD pattern corresponding to the fully hydrated material was recovered (Figure S4).

In an attempt to exploit the internal surface area of Mg-CUK1L, we next studied the adsorption of larger liquid and solid hydrocarbons. Mg-CUK-1 was able to selectively adsorb pxylene over and p-divinylbenzene over mixtures of other isomers because the o- and m-isomers have larger critical diameters.[4a] The significantly larger channel openings in Mg-CUK-1L should permit entry of the larger isomers. Immersion of dehydrated crystals in o-xylene resulted in new high-angle reflections in the PXRD pattern (Figure S4). SCXRD analysis revealed that the channels were filled with o-xylene (Figure S5 & Table S1). MgCUK-1L⊂3(o-xylene) retained the same space group to the dehydrated material and o-xylene molecules were packed based on host-guest π-π interactions, as well as short guest-guest CH-π contacts (Figure S5).

Based on this encouraging result, we explored the application of Mg-CUK-1L as a host for the capture and crystallographic determination of larger organic molecules. Fujita and Yaghi have demonstrated absolute configurational resolution of chiral organic molecules constrained inside MOF micropores.[11] There is also interest in the isolation of photoisomerizable molecules inside MOFs to probe their properties in the solid-state. Ruschewitz used MIL-68 to adsorb azobenzene (AzB; $(C_6H_5N)_2$) from vapor, but only achieved 30% loading.[12] Zhou reported a MOF with azo linkages in the framework that underwent reversible trans-cis inversion upon irradiation.[13] Heinke later reported loading of AzB into HKUST-1 from ethanol, but this method did not produce crystals suitable for SCXRD.[14]

The robustness of Mg-CUK-1L enabled us to directly load AzB in Mg-CUK-1L by heating dehydrated crystals in a neat AzB melt at 80 °C, without losing crystallinity. The structure of Mg-CUK1L⊂2AzB was solved in the triclinic space group, (P1, Z = 2; Figures S5-6 & Table S1). AzB molecules adopt thermodynamically favored trans configurations and the C−N=N−C bond angles are unremarkable (Figure 4). Given the aromatic apolar nature of AzB, the closest host-guest interactions are formed

with the aromatic moieties of the channel walls.[4a-d] The AzB molecules are closely packed in a 2×2 end-to-end arrangement (Figure 4B), with no free space remaining in the channels (Figure 4C).

Next, we assessed if photo-isomerization to the cis form was hindered in the solid-state. UV-vis spectra of hydrated Mg-CUK1L revealed no absorption bands between 300−800 nm and a strong band below 250 nm corresponding to MOF-based metalligand charge transfer. Irradiation of the same sample at 320 or 460 nm for 60 s resulted in no spectral changes (Figure S7). In contrast, the UV-vis spectrum of the AzB-loaded material showed two characteristic absorbances ca. 317.5 nm and 439 nm, corresponding to and $\pi \rightarrow \pi*$ $n \rightarrow \pi*$ transitions of AzB, respectively (Figures S8 & S9).[15] Irradiation of Mg-CUK1L⊂2AzB at 320 nm and collection of emission spectra at regular intervals revealed significant diminishment of the band at 317 nm after <30 s, accompanied by an increase in the band ca. 439 nm due to cis-AzB (Figures 5A & S11). The observed 'soft crystalline,'[16] flexible nature of MgCUK-1L allows the framework to accommodate the trans-to-cis conversion. Isomerization back to the trans state was achieved by irradiation at 460 nm for 30 s; the process was repeated over multiple cycles without loss of integrated intensity, indicating full reversibility (Figure 5A; inset).

To further understand the trans-cis photo-isomerization and to determine the origin of the loss of UV-vis response between 310- 320 nm, DFT calculations were performed to model the optical transitions (Supporting Information). The calculated UV-Vis spectra for cis- and trans-AzB molecules loaded in Mg-CUK-1L are in close agreement with the experimental observations (Figure 5B). DFT of the trans-AzB-loaded MOF predicted a characteristic absorption band at 295 nm that was diminished for cis-AzB, in-line with the experimental findings. Independent UV-Vis spectra calculated for isolated AzB molecules in both configurations (Figure S12) showed a strong response at 315 nm for trans-AzB corresponding to a transition; the same $\pi \rightarrow \pi*$ response was weak for cis-AzB.

The measured rate of thermal cis-to-trans relaxation of MgCUK-1L⊂2AzB after irradiation at 320 nm at 298 K in the dark was slow (t½ = 6.6 h; Figure S13). This enabled PXRD studies of the cis form immediately after irradiation at 320 nm, which revealed retention of crystallinity but no distinguishable differences in the bulk diffraction compared to the trans form. Furthermore, the simulated PXRD pattern for the cis-AzB form obtained from DFT studies is in excellent agreement (Figure S14). This is reasonable since the major reflections are due to the (ordered) host framework atoms.

Together with the DFT-predicted single crystal structure of cisAzB molecules in Mg-CUK-1L (Figure S15), it is apparent that trans-AzB molecules undergo reversible photo-isomerization within the Mg-CUK-1L channels. Further studies using this material in water sorption and the sorption of chiral molecules are currently under way in our lab.

Supporting Information

Experimental procedures and spectral data. CCDC numbers 1965418-1965421 contain the CIF data for structures.

Corresponding Author

E.L.Q.: emilyque@cm.utexas.edu; G.H.: henkelman@utexas.edu; S.M.H.: smh@cm.utexas.edu.

Notes

The authors declare no competing financial interests.

Acknowledgement

The authors thank Dr. Vince M. Lynch for X-ray assistance, the Texas Advanced Computing Centre (TACC) for computational resources, the Welch Foundation (F-1738, S.M.H.; F-1883, E.L.Q.; F-1841, G.H.) and ConTex for funding.

References

1. (a) Nandasiri, M. I.; Jambovane, S. R.; McGrail, B. P.; Schaef, H. T.; Nune, S. K. Adsorption, separation, and catalytic properties of densified metal-organic frameworks. *Coord. Chem. Rev.* **2016**, *311*, 38-52; (b) Chen, C.; Jiang, Q.; Xu, H.; Lin, Z. Highly efficient synthesis of a moisture-stable nitrogen-abundant metal-organic framework (MOF) for large-scale CO_2 capture. *Ind. Eng. Chem. Res.* **2019**, *58*, 1773-1777.

2. Kim, H.; Yang, S.; Rao, S. R.; Narayanan, S.; Kapustin, E. A.; Furukawa, H.; Umans, A. S.; Yaghi, O. M.; Wang, E. N. Water harvesting from air with metal-organic frameworks powered by natural sunlight. *Science* **2017**, *356*, 430-434.

3. (a) Borjigin, T.; Sun, F.; Zhang, J.; Cai, K.; Ren, H.; Zhu, G. A microporous metal-organic framework with high stability for GC separation of alcohols from water. *Chem. Comm.* **2012**, *48*, 7613- 7615; (b) Zhang, H.; Xiao, R.; Song, M.; Shen, D.; Liu, J. Hydrogen production from bio-oil by chemical looping reforming - Characteristics of the synthesized metal organic frameworks for CO_2 removal. *J. Therm. Anal. Calorim.* **2014**, *115*, 1921-1927; (c) Wang, C.; Liu, X.; Demir, N. K.; Chen, J. P.; Li, K. Applications of water stable metal-organic frameworks. *Chem. Soc. Rev.* **2016**, *45*, 5107- 5134.

4. (a) Saccoccia, B.; Bohnsack, A. M.; Waggoner, N. W.; Cho, K. H.; Lee, J. S.; Hong, D.; Lynch, V. M.; Chang, J.; Humphrey, S. M. Separation of p-divinylbenzene by selective room-temperature adsorption inside Mg-CUK-1 prepared by aqueous microwave synthesis. *Angew. Chem. Int. Ed.* **2015**, *54*, 5394-5398; (b) Humphrey, S. M.; Chang, J.-S.; Jhung, S. H.; Yoon, J. W.; Wood, P. T. Porous cobalt(II)-organic frameworks with corrugated walls: Structurally robust gas-sorption materials. *Angew. Chem. Int. Ed.* **2007**, *46*, 272-275; (c) Yoon, J. W.; Jhung, S. H.; Hwang, Y. K.; Humphrey, S. M.; Wood, P. T.; Chang, J.-S. Gas-sorption selectivity of CUK-1: a porous coordination solid made of cobalt(II) and pyridine-2,4-dicarboxylic acid. *Adv. Mater.* **2007**, *19*, 1830-1834; (d) Lee, J. S.; Yoon, J. W.; Mileo, P. G. M.; Cho, K. H.; Park, J.;Kim, K.; Kim, H.; Lange, M. F.; Kapteijn, F.; Maurin, G.; Humphrey, S. M.; Chang, J.-S. Porous metal-organic framework CUK-1 for adsorption heat allocation toward green applications of natural refrigerant water. *ACS Appl. Mater. Inter.* **2019**, *11*, 25778-2578; (e) Sánchez-González, E.; Mileo, P. G. M.; Sagastuy-Breña, M.; Álvarez, J. R.; Reynolds, J. E.; Villarreal, A.; Gutiérrez-Alejandre, A.; Ramírez, J.; Balmaseda, J.; González-Zamora, E.; Maurin, G.; Humphrey, S. M.; Ibarra, I. A. Highly reversible sorption of H_2S and CO_2 by an environmentally friendly Mg-based MOF. *J. Mater. Chem. A* **2018**, *6*, 16900-16909.

5. (a) Yaghi, O. M.; Kalmutzki, M. J.; Diercks, C. S. *Introduction to Reticular Chemistry: Metal-Organic Frameworks and Covalent Organic Frameworks*, **2019**, Wiley-VCH; (b) Zhao, D.; Timmons, D. J.; Yuan, D.; Zhou, H.-C. Tuning the topology and functionality of metal-organic frameworks by ligand design.

Acc. Chem. Res. **2011**, *44*, 123-133; (c) Garibay, S. J.; Cohen, S. M. Isoreticular synthesis and modification of frameworks with the UiO-66 topology. *Chem. Comm.* **2010**, *46*, 7700-7702.

6. Eddaoudi, M.; Kim, J.; Rosi, N.; Vodak, D.; Wachter, J.; O'Keeffe, M.; Yaghi, O. M. Systematic design of pore size and functionality in isoreticular MOFs and their application in methane storage. *Science* **2002**, *295*, 469-472.

7. Spek, A. L. Structure validation in chemical crystallography. *Acta Cryst.* **2009**, *65*, 148-155.

8. (a) Choi, H. J.; Dincă, M.; Long, J. R. Broadly hysteretic H_2 adsorption in the microporous metal-organic framework Co(1,4- benzenedipyrazolate). *J. Am. Chem. Soc.* **2008**, *130*, 7848-7850; (b) Ravikovitch, P. I.; Domhnaill, S. C. Ó.; Neimark, A. V.; Schüth, F.; Unger, K. K. Capillary hysteresis in nanopores: theoretical and experimental studies of nitrogen adsorption on MCM-41. *Langmuir* **1995**, *11*, 4765-4772.

9. (a) Guo, Z.; Li, G.; Zhou, L.; Su, S.; Lei, Y.; Dang, S.; Zhang, H. Magnesium-based 3D metal-organic framework exhibiting hydrogen-sorption hysteresis. *Inorg. Chem.* **2009**, *48*, 8069-8071; (b) Mulfort, K. L.; Farha, O. K.; Malliakas, C. D.; Kanatzidis, M. G.; Hupp, J. T. An interpenetrated framework material with hysteretic CO2 uptake. *Chem. Eur. J.* **2010**, *16*, 276-281; (c) Zhong, D.; Zhang, W.; Cao, F.; Jiang, L.; Lu, T. A three-dimensional microporous metal-organic framework with large hydrogen sorption hysteresis. *Chem. Commun.* **2011**, *47*, 1204-1206.

10. Mason, J. A.; Oktawiec, J.; Taylor, M. K.; Hudson, M. R.; Rodriguez, J.; Bachman, J. E.; Gonzalez, M. I.; Cervellino, A.; Guagliardi, A.; Brown, C. M.; Llewellyn, P. L.; Masciocchi, N.; Long, J. R. Methane storage in flexible metal-organic frameworks with intrinsic thermal management. *Nature*, **2015**, *527*, 357-361.

11. (a) Lee, S.; Kapustin, E. A.; Yaghi, O. M. Coordinative alignment of molecules in chiral metal-organic frameworks. *Science* **2016**, *353*, 808-811; (b) Yan, K.; Dubey, R.; Arai, T.; Inokuma, Y.; Fujita, M. Chiral crystalline sponges for the absolute structure determination of chiral guests. *J. Am. Chem. Soc.* **2017**, *139*, 11341-11344.

12. Hermann, D.; Emerich, H.; Lepski, R.; Schaniel, D.; Ruschewitz, U. Metal-organic frameworks as hosts for photochromic guest molecules. *Inorg. Chem.* **2013**, *52*, 2744-2749.

13. Park, J.; Sun, L. B.; Chen, Y. P.; Perry, Z.; Zhou, H. C. Azobenzene-functionalized metal-organic polyhedra for the optically responsive capture and release of guest molecules. *Angew. Chem. Int. Ed.* **2014**, *53*, 5842-5846.

14. Mueller, K.; Wadhwa, J.; Malhi, S. J.; Schoettner, L.; Welle, A.; Schwartz, H.; Hermann, D.; Ruschewitz, U.; Heinke, L. Photoswitchable nanoporous films by loading azobenzene in metalorganic frameworks of type HKUST-1. *Chem. Comm.* **2017**, *53*, 8070-8073.

15. (a) Bandara, H. M. D.; Burdette, S. C. Photoisomerization in different classes of azobenzene. *Chem. Soc. Rev.* **2012**, *41*, 1809- 1825; (b) Schultz, T.; Quenneville, J.; Levine, B.; Toniolo, A.; Martínez, T. J.; Lochbrunner, S.; Schmitt, M.; Shaffer, J. P.; Zgierski, M. Z.; Stolow, A. Mechanism and dynamics of azobenzene photoisomerization. *J. Am. Chem. Soc.* **2003**, *125*, 8098-8099.

16. Horike, S.; Shimomura, S.; Kitagawa, S. Soft porous crystals. Nature Chem. **2009**, 1, 695-704.

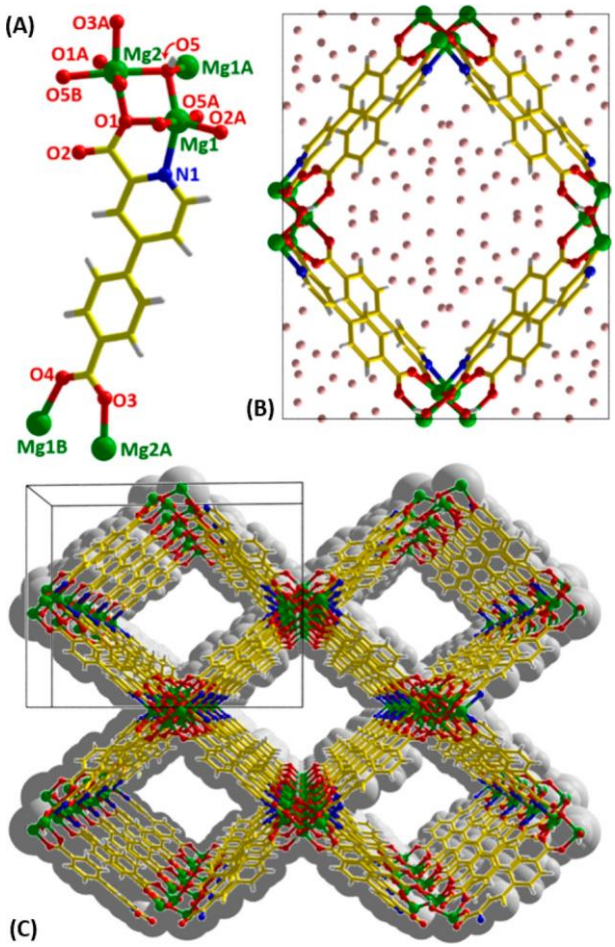

Figure 1. (A) Asymmetric unit of Mg-CUK-1L. (B) Unit cell viewed in the crystallographic ac-plane with solvent O-atoms drawn in pink. (C) Extended view of CUK-1L showing 1-D channels; space filling model is shown in grey.

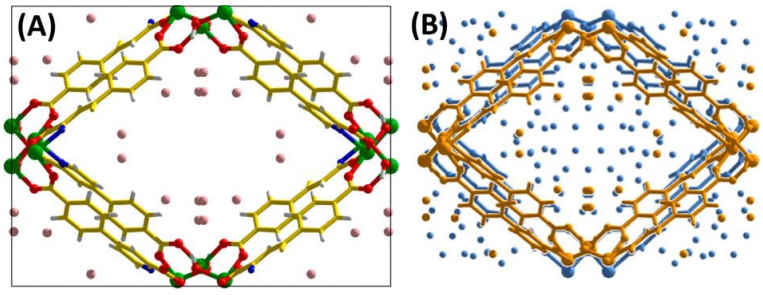

Figure 2. (A) Unit cell of dehydrated Mg-CUK-1L. (B) Super-imposition of unit cells for the hydrated (blue) and dehydrated (orange) crystal structures.

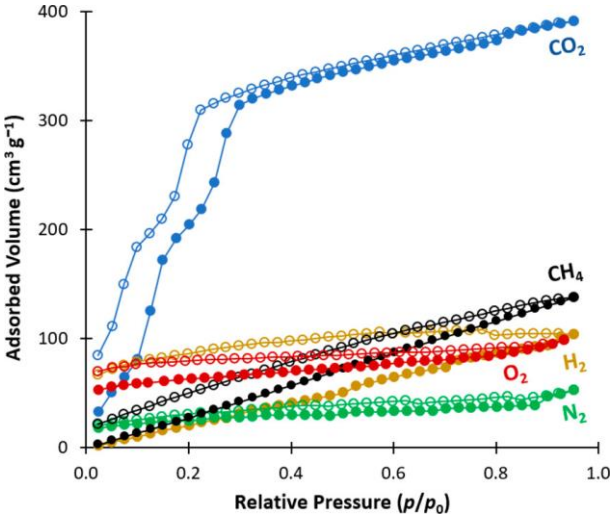

Figure 3. Adsorption-desorption isotherms for gases in Mg-CUK-1L: N_2, O_2 at & H_2 at 77 K, CH_4 & CO_2 at 196 K; closed circles = adsorption, open circles = desorption.

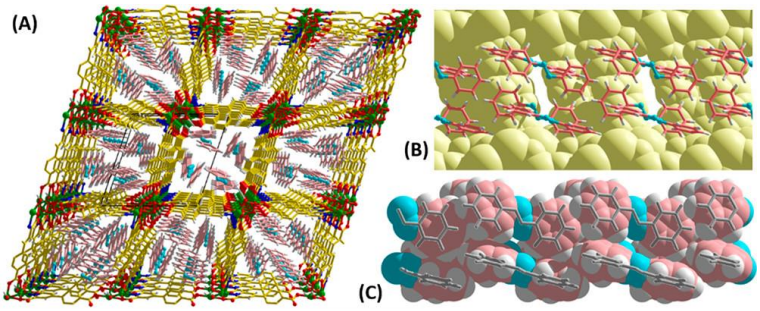

Figure 4. (A) Packing view of Mg-CUK-1L⊂2AzB in the bc-plane; AB molecules are drawn in pink (C) and cyan (N). (B) Cross-sectional view of a single AB-loaded channel. (C) Space-filling representation of AB molecules with the host framework removed, showing close packing of AB molecule aligned in end-to-end fashion.

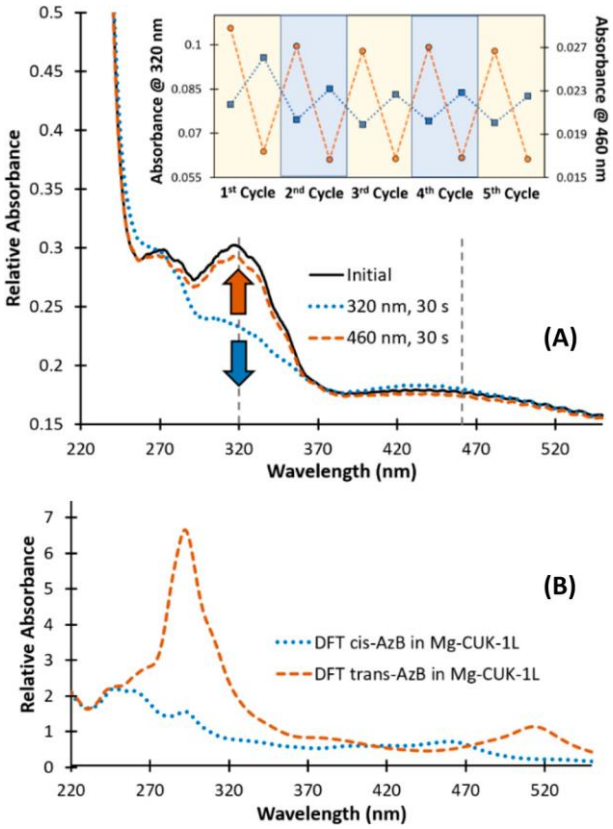

Figure 5. (A) In situ UV-vis spectra for Mg-CUK-1L⊂2AB showing fast and reversible loss of the trans-N_2 absorption ca. 320 nm. Inset: relative absorbances at 320 and 460 nm upon cycling. (B) DFT-calculated absorbance spectra for MgCUK-1L loaded with cis- and trans-AzB.